Relative intensity noise properties of quantum dot lasers

Jianan Duan[a,b,*], Xing-Guang Wang[b], Yue-Guang Zhou[b], Cheng Wang[b], and Frédéric Grillot[a,c]

[a]LTCI, Télécom ParisTech, Université Paris-Saclay, Paris, France
[b]School of Information Science and Technology, ShanghaiTech University, Shanghai, China
[c]Center for High Technology Materials, University of New-Mexico, Albuquerque, NM, USA

ABSTRACT

In this work, we theoretically investigate the relative intensity noise (RIN) properties of quantum dot (QD) lasers through a rate equation model including the Langevin noises and the contribution from the off resonance energy levels. It is shown that the carrier noise significantly enhances the RIN which can be further reduced by properly controlling the energy separation between the first excited and the ground states. In addition, simulations also unveil that the RIN of QD lasers is rather temperature independent which is of prime importance for the development of power efficient light sources. Overall, these results indicate that QD lasers are excellent candidates for the realization of ultra-low noise oscillators hence being advantageous for fiber optics communication networks, short reach optical interconnects and integrated photonics systems.

Keywords: Semiconductor lasers, Quantum dots, Relative intensity noise

1. INTRODUCTION

The relative intensity noise (RIN) of semiconductor lasers degrades the signal-to-noise ratio (SNR) and increases the bit-error rate of optical signals hence setting a limit of a high-speed communication system.[1,2] A low RIN floor across the operating range is usually required to achieve a large SNR. System limitations due to poor SNR can be compensated by increasing the bias current of the laser source but at the price of a larger energy consumption. In radar related applications, the intensity noise of the laser is also of first importance since it is expected to be closed to that of the shot noise over a bandwidth ranging up to 20 GHz.[3] Compared to quantum well (QW) lasers, significant breakthroughs have been achieved by using quantum dots (QD) as gain media. QD lasers can produce energy- and cost-efficient devices with outstanding temperature stability, low threshold current, reduced phase and intensity noises and richer complex dynamics.[4,5] For instance, recent works have shown that the sole ground state (GS) emission makes QD lasers highly insensitive to external optical perturbations whereas those emitting exclusively on the first excited state (ES) exhibit a plethora of nonlinear dynamical behaviors.[6–8] As for the intensity noise, prior works have experimentally shown a RIN level as low as -160 dB/Hz on both InAs/GaAs and InAs/InP QD lasers,[9,10] whereas it was found slightly higher e.g. from - 140 dB/Hz to -150 dB/Hz in QD lasers directly grown on silicon.[11] The RIN of QD lasers has been theoretically investigated however being significantly underestimated because prior models were not taken into account the carrier noise[12] or when doing so, it was only that from the GS level.[13] Therefore, this work goes a step forward by numerically reporting on the RIN of QD lasers analyzed by a rate equation model incorporating the Langevin noises associated with both spontaneous emission and carrier noise through the contributions of both resonance and off-resonance energy levels. It is shown that the carrier noise in both the GS and ES significantly enhances the RIN, while that in the carrier reservoir (RS) does not, hence showing that the inclusion of the ES contribution is required for getting an accurate description of the laser intensity noise. On the other hand, the energy separation between ES and GS is found to have a strong impact on the RIN meaning that a large energy separation namely a small vertical coupling is more suitable for RIN reduction due to the suppression of the carrier noise contribution of the ES. Finally, simulations unveil that the RIN of QD lasers is rather temperature independent, which is also of vital importance for stable and energy efficient low noise QD oscillators.

* Corresponding author: jianan.duan@telecom-paristech.fr

2. NUMERICAL MODEL

QDs are assumed to be neutral hence electrons and holes are treated as electron-hole pairs meaning that the system only consists of excitonic energy states. Carriers are supposed to be directly injected from the contacts into the RS, so the carrier dynamics in the barrier are not taken into account. The model is based on the assumption that the active region includes only one QD ensemble incorporate a two-fold degenerate GS as well as a four-fold degenerate ES. As shown in Figure 1, the carriers are at first captured from the RS into the ES with capture time τ_{ES}^{RS}, and then relax from the ES down to the GS with a relaxation time τ_{GS}^{ES}. On the other hand, some carriers can also be thermally reemitted from the ES to the RS with an escape time τ_{RS}^{ES}, which is governed by the Fermi distribution for the quasi-thermal equilibrium without external excitation. Similar dynamic behavior is followed by the carrier population on the GS level with regards to the ES carriers with an escape time τ_{ES}^{GS}. The differential rate equations describing carrier and photon dynamics are expressed as:[14]

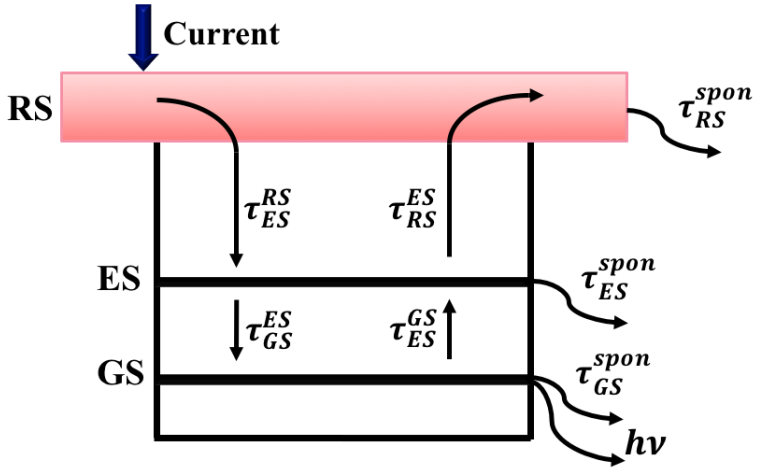

Figure 1. Schematic of the electronic structure and carrier dynamics in the InAs/InP QD structure.

$$\frac{dN_{RS}}{dt} = \frac{I}{q} + \frac{N_{ES}}{\tau_{RS}^{ES}} - \frac{N_{RS}}{\tau_{ES}^{RS}}(1-\rho_{ES}) - \frac{N_{RS}}{\tau_{RS}^{spon}} + F_{RS} \tag{1}$$

$$\frac{dN_{ES}}{dt} = \left(\frac{N_{RS}}{\tau_{ES}^{RS}} + \frac{N_{GS}}{\tau_{ES}^{GS}}\right)(1-\rho_{ES}) - \frac{N_{ES}}{\tau_{GS}^{ES}}(1-\rho_{GS}) - \frac{N_{ES}}{\tau_{RS}^{ES}} - \frac{N_{ES}}{\tau_{ES}^{spon}} + F_{ES} \tag{2}$$

$$\frac{dN_{GS}}{dt} = \frac{N_{ES}}{\tau_{GS}^{ES}}(1-\rho_{GS}) - \frac{N_{GS}}{\tau_{ES}^{GS}}(1-\rho_{ES}) - \Gamma_p v_g g_{GS} S_{GS} - \frac{N_{GS}}{\tau_{GS}^{spon}} + F_{GS} \tag{3}$$

$$\frac{dS_{GS}}{dt} = \left(\Gamma_p v_g g_{GS} - \frac{1}{\tau_p}\right) S_{GS} + \beta_{sp}\frac{N_{GS}}{\tau_{GS}^{spon}} + F_S \tag{4}$$

where I is the bias current, q the elementary charge, $N_{RS,ES,GS}$ the carrier populations in the RS, ES, and GS, respectively and S_{GS} the photon number in the GS level. It is worth noting that the model only considers the stimulated emission from the GS transition and that from the ES is not taken into account. In addition, carriers also recombine spontaneously with a spontaneous emission times $\tau_{RS,ES,GS}^{spon}$. Finally, it is noted that $\rho_{ES,GS}$ correspond to the carrier occupation probabilities in the ES and GS, while Γ_p is the optical confinement factor, τ_p the photon lifetime, v_g the group velocity and β_{sp} the spontaneous emission factor in the lasing mode.

Modeling of the RIN is conducted through the inclusion of the Langevin noise sources related to both carrier and spontaneous emission noises.[15] Thus, $F_{RS,ES,GS}$, and F_S represent the carrier noise and the photon noise respectively. Moreover, the correlation strength of two Langevin noise sources is defined as $\langle F_i(t)F_j(t')\rangle = U_{ij}\delta(t-t')$, where indexes i,j refer to RS, ES, GS and S with U_{ij} the diffusion coefficients between two noise

sources which are delta-correlated. Based on the steady-state solutions from (1) - (4), the diffusion coefficients of all the Langevin noise source are derived as:[1]

$$U_{RSRS} = 2 \times \left(\frac{N_{RS}}{\tau_{ES}^{RS}}(1-\rho_{ES}) + \frac{N_{RS}}{\tau_{RS}^{spon}} \right) \tag{5}$$

$$U_{ESES} = 2 \times \left(\frac{N_{RS}}{\tau_{ES}^{RS}} + \frac{N_{GS}}{\tau_{ES}^{GS}} \right)(1-\rho_{ES}) \tag{6}$$

$$U_{GSGS} = 2 \times \left[\frac{N_{ES}}{\tau_{GS}^{ES}}(1-\rho_{GS}) - \Gamma_p v_g g_{GS} S_{GS} + \beta_{sp} \frac{N_{GS}}{\tau_{GS}^{spon}} S_{GS} \right] \tag{7}$$

$$U_{RSES} = -\left[\frac{N_{RS}}{\tau_{ES}^{RS}}(1-\rho_{ES}) + \frac{N_{ES}}{\tau_{RS}^{ES}} \right] \tag{8}$$

$$U_{ESGS} = -\left[\frac{N_{GS}}{\tau_{ES}^{GS}}(1-\rho_{ES}) + \frac{N_{ES}}{\tau_{GS}^{ES}}(1-\rho_{GS}) \right] \tag{9}$$

$$U_{GSS} = -\left[2\beta_{sp} \frac{N_{GS}}{\tau_{GS}^{spon}} S_{GS} - \Gamma_p v_g g_{GS} S_{GS} \right] \tag{10}$$

$$U_{SS} = 2 \times \beta_{sp} \frac{N_{GS}}{\tau_{GS}^{spon}} S_{GS} \tag{11}$$

The above Langevin noise sources perturb the laser system away from its steady-state condition. Linearizing the rate equations (1) - (4), the differential rate equations can be expressed in the frequency domain such as:

$$\begin{bmatrix} \gamma_{11}+j\omega & -\gamma_{12} & 0 & 0 & 0 \\ -\gamma_{21} & \gamma_{22}+j\omega & -\gamma_{23} & 0 & 0 \\ 0 & -\gamma_{32} & \gamma_{33}+j\omega & -\gamma_{34} & 0 \\ 0 & 0 & -\gamma_{43} & \gamma_{44}+j\omega & 0 \end{bmatrix} \times \begin{bmatrix} \delta N_{RS} \\ \delta N_{ES} \\ \delta N_{GS} \\ \delta S_{GS} \end{bmatrix} = \begin{bmatrix} F_{RS} \\ F_{ES} \\ F_{GS} \\ F_S \end{bmatrix} \tag{12}$$

with

$$\begin{aligned} &\gamma_{11} = \frac{1-\rho_{ES}}{\tau_{ES}^{RS}} + \frac{1}{\tau_{RS}^{spon}}; \gamma_{12} = \frac{1}{\tau_{RS}^{ES}} + \frac{1}{4N_B}\frac{N_{RS}}{\tau_{ES}^{RS}}; \gamma_{21} = \frac{1-\rho_{ES}}{\tau_{ES}^{RS}}; \gamma_{23} = \frac{1-\rho_{ES}}{\tau_{ES}^{GS}} + \frac{1}{2N_B}\frac{N_{ES}}{\tau_{GS}^{ES}}; \\ &\gamma_{22} = \frac{1-\rho_{GS}}{\tau_{GS}^{ES}} + \frac{1}{\tau_{RS}^{ES}} + \frac{1}{\tau_{ES}^{spon}} + \frac{1}{4N_B}\left(\frac{N_{RS}}{\tau_{ES}^{RS}} + \frac{N_{GS}}{\tau_{ES}^{GS}} \right); \gamma_{32} = \frac{1-\rho_{GS}}{\tau_{GS}^{ES}} + \frac{1}{4N_B}\frac{N_{GS}}{\tau_{ES}^{GS}}; \\ &\gamma_{33} = \frac{1-\rho_{ES}}{\tau_{ES}^{GS}} + \frac{1}{\tau_{GS}^{spon}} + \frac{1}{2N_B}\frac{N_{ES}}{\tau_{GS}^{ES}} + \Gamma_p v_g a_{GS} S_{GS}; \gamma_{34} = -\Gamma_p v_g g_{GS} + \Gamma_p v_g a_p S_{GS}; \\ &\gamma_{43} = \Gamma_p v_g a_{GS} S_{GS} + \frac{\beta_{sp}}{\tau_{GS}^{spon}}; \gamma_{44} = \frac{1}{\tau_p} - \Gamma_p v_g g_{GS} + \Gamma_p v_g a_p S_{GS}; \end{aligned} \tag{13}$$

Where N_B is the total dot number, the gain variation is determined by both the carrier and photon density variations: $dg_{GS} = a_{GS} dN_{GS} - a_p dS_{GS}$, with a_{GS} refers to GS differential gain and a_p deals with the gain is compressed at high photon densities. Therefore, following Cramer's rule, the RIN of GS in the QD laser is calculated by:

$$RIN(\omega) = \frac{|\delta S_{GS}(\omega)|^2}{S_{GS}^2} \tag{14}$$

with $\delta S_{GS}(\omega)$ the photon number variation in the frequency domain and S_{GS} presents the average photon number. The laser under study is an InAs/InP QD laser emitting near 1550 nm and exhibiting a threshold current (I_{th}) of 48 mA at room temperature. All material and optical parameters of the QD laser used in the simulations are listed in Table 1 in appendix,[14] unless stated otherwise.

3. NUMERICAL RESULTS AND DISCUSSION

Figure 2 unveils the contribution of carrier noise ($F_{RS,ES,GS}$) to the RIN spectra of the QD laser at different bias currents of $2 \times I_{th}$, $3 \times I_{th}$ and $4 \times I_{th}$, respectively. The RIN remains stable at low frequencies typically below 1.0 GHz, while it strongly decreases above the resonance frequency peak of the QD laser. It is noted that the random division of reflected and transmitted photons at the cavity facets which should result in a noise floor at high frequencies in the RIN spectrum is not included in the calculations.[1] Compared with the RIN spectra without $F_{RS,ES,GS}$ (dot curves), the inclusion of the $F_{RS,ES,GS}$ (solid curves) significantly strengthen the magnitude of the RIN over the frequency range especially at low frequencies (< 1.0 GHz). For instance, the RIN extracted at 1 MHz at $2 \times I_{th}$ is enhanced from -150 dB/Hz to -140 dB/Hz when the carrier noise is included.

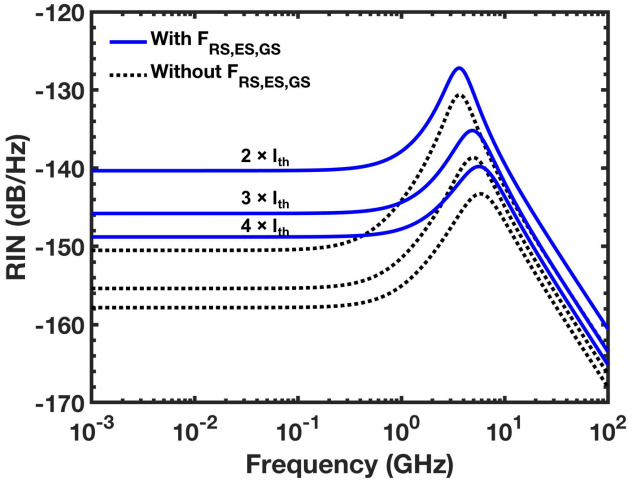

Figure 2. Contribution of $F_{RS,ES,GS}$ to the RIN at bias currents of $2 \times I_{th}$, $3 \times I_{th}$ and $4 \times I_{th}$ respectively. The solid lines are with carrier noise while the dot lines are not.

Figure 3 depicts the bias current dependence of the damping factor and the resonance frequency of the RIN spectra including the $F_{RS,ES,GS}$. At a higher bias current, both the damping factor and the resonance frequency are increased which is in agreement with Figure 2 showing that the resonance frequency peak scales up with the bias current while its amplitude is reduced.

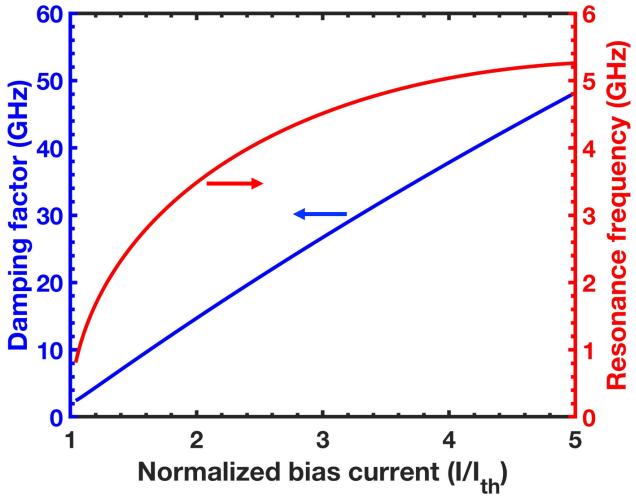

Figure 3. The bias current dependence of the damping factor and the resonance frequency of the RIN spectra including the $F_{RS,ES,GS}$.

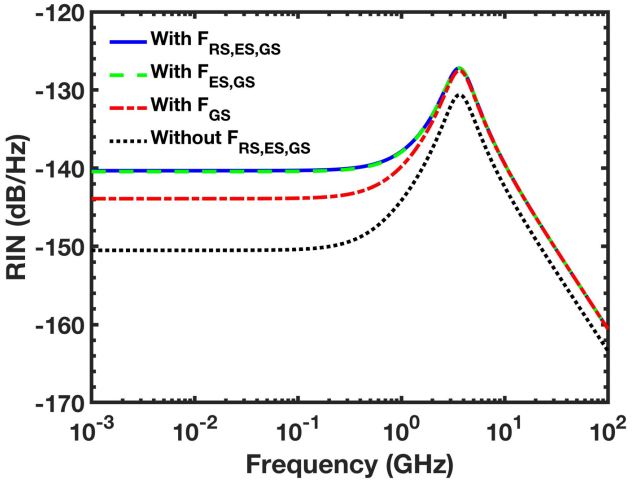

Figure 4. Calculated RIN spectra at $2\times I_{th}$ for cases including the carrier noise sources $F_{RS,ES,GS}$, $F_{ES,GS}$, F_{GS} and without $F_{RS,ES,GS}$.

The contribution of the carrier noise in each state to the laser RIN is now illustrated in Figure 4 at $2 \times I_{th}$ for cases with $F_{RS,ES,GS}$ (solid line), $F_{ES,GS}$ (dash line), F_{GS} (dash-dot line) and without $F_{RS,ES,GS}$ (dot line), respectively. In comparison with the RIN spectrum without the carrier noise ($F_{RS,ES,GS}$), F_{GS} enhances the RIN amplitude over the whole frequency range, while F_{ES} only increases the RIN at frequencies below the resonance frequency. In particular, it has to be noted that the contribution of F_{RS} remains perfectly negligible.

As F_{GS} and F_{ES} clearly dominate the laser intensity noise, simulations unveil that it can be compressed by controlling the ES-GS energy separation ΔE_{GS}^{ES}, namely, the vertical coupling between ES and GS. In the simulation, the RS-GS energy separation is fixed such as $\Delta E_{GS}^{RS} = 3\times\Delta E_{GS}^{ES}$ while the carrier capture and relaxation times are supposed to be constant hence independent of the energy separation.[16] However, since the threshold current varies with the ES-GS energy separation, it is better to fix the photon number for comparing the impact of the energy separation ΔE_{GS}^{ES} on the RIN. Figure 5 depicts the RIN spectra when assuming for example a pretty large variation of ΔE_{GS}^{ES} from 50 meV to 160 meV with a step of 10 meV. The photon number is still at 2×10^5 which corresponds to a pumping condition already far from the laser threshold for which a typical

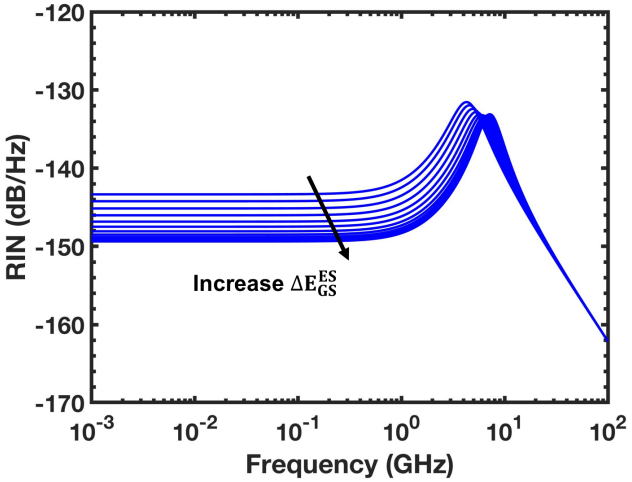

Figure 5. The RIN spectra plotted as a function of the ES-GS energy separation increasing from 50 meV to 160 meV with a step of 10 meV and at a fixed photon number of 2×10^5.

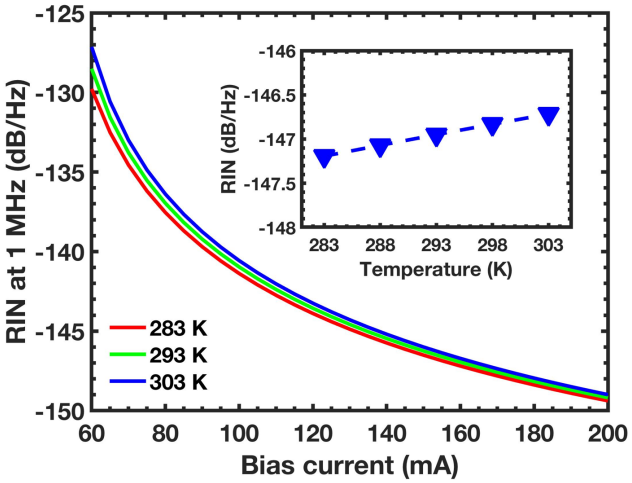

Figure 6. Calculated RIN at 1 MHz as a function of the bias current at 283 K, 293 K and 303 K, respectively. The inset shows the RIN values plotted as a function of temperature assuming a bias current of 160 mA.

photon number of 1×10^3 usually occurs. Simulation proves that a large ES-GS energy separation compresses the low-frequency part of the RIN before the resonance frequency peak. For instance, the RIN at 1 MHz is found to be reduced by as much as 6 dB from -143 dB/Hz at 50 meV down to -149 dB/Hz at 160 meV. However, the RIN tends to an intrinsic limit value associated with the F_{GS} when further increasing ΔE_{GS}^{ES}, since the ES-GS energy separation can only minimize the contribution from the ES. As a consequence, a large ES-GS energy separation, namely, a small vertical coupling between the ES and the GS is more beneficial for low intensity noise operation in QD lasers due to the reduced carrier noise from the ES. This also proves that the inclusion of ES contribution in the model is necessary for accurately characterizing the RIN properties in QD lasers.

The effect of the temperature on the RIN of QD lasers is now investigated. This study is particularly motivated by our previous work in which a rather temperature insensitive behavior was also unveiled between 283 K and 303 K for the optical linewidth of InAs/InP QD lasers.[17] Figure 6 presents the evolution of the calculated low-frequency RIN (at 1 MHz) as a function of the bias current between 283 K and 303 K. The RIN is at first drastically reduced near the threshold and a further decrease is achieved at high bias currents owing to the strong damping factor. In addition, for a bias current of 160 mA, the inset also shows that the value of the RIN increases from - 147.2 dB/Hz at 283 K to - 147 dB/Hz at 293 K, and -146.7 dB/Hz at 303 K with a variation of 0.5 dB/Hz over the temperature range of 20 K. These results demonstrate the RIN of QD lasers is pretty stable over temperature variations.

4. CONCLUSIONS

To sum, this work shows that the carrier noise in the ES and GS significantly enhances the RIN, while that in the RS is negligible hence showing that the inclusion of the ES contribution is of paramount importance for a better and accurate analysis of the intensity noise. Since the energy separation between ES and GS is found to have a strong impact on the RIN, hence a large energy separation namely a small vertical coupling is more suitable for low intensity noise operation due to the suppression of the carrier noise in the ES of QD lasers. In the end, simulations also unveil that the RIN of QD lasers is rather temperature independent, which is in encouraging for the realization of stable and power efficient light sources. Overall, results show that QD lasers can be used as ultra-low noise oscillators not only in fiber optic communication networks but also for short reach optical interconnects in high performance computers and in board-to-board and chip-to-chip integrated photonic systems.

ACKNOWLEDGMENTS

The authors want to thank the Institut Mines-Télécom and the financial support from Shanghai Pujiang Program. Jianan Duan's work is supported by China Scholarship Council. Cheng Wang's work is supported by National Natural Science Foundation of China (61804095) and also by Shanghai Pujiang Program (17PJ1406500).

APPENDIX A. MATERIAL AND OPTICAL PARAMETERS OF QD LASER

Table 1. Material and optical parameters of the InAs/InP(311B) QD laser.

Symbol	Description	Value
E_{RS}	RS transition energy	0.97 eV
E_{ES}	ES transition energy	0.87 eV
E_{GS}	GS transition energy	0.82 eV
τ_{ES}^{RS}	RS to ES capture time	6.3 ps
τ_{GS}^{ES}	ES to GS relaxation time	2.9 ps
τ_{RS}^{ES}	ES to RS escape time	2.7 ns
τ_{ES}^{GS}	GS to ES escape time	10.4 ps
τ_{RS}^{spon}	RS spontaneous emission time	0.5 ns
τ_{ES}^{spon}	ES spontaneous emission time	0.5 ns
τ_{GS}^{spon}	GS spontaneous emission time	1.2 ns
τ_p	Photon lifetime	4.1 ps
T_2	Polarization dephasing time	0.1 ps
β_{sp}	Spontaneous emission factor	1×10^{-4}
a_{GS}	GS Differential gain	5.0×10^{-15} cm^2
a_{ES}	ES Differential gain	10×10^{-15} cm^2
a_{RS}	RS Differential gain	2.5×10^{-15} cm^2
ξ	Gain compression factor	2.0×10^{-16} cm^3
Γ_p	Optical confinement factor	0.06
N_B	Total dot number	1×10^7
D_{RS}	Total RS state number	4.8×10^6
V_B	Active region volume	5×10^{-11} cm^3
V_{RS}	RS region volume	1×10^{-11} cm^3

REFERENCES

[1] Coldren, L. A., Corzine, S. W., and Mashanovitch, M. L., [*Diode lasers and photonic integrated circuits*], vol. 218, John Wiley & Sons (2012).

[2] Norman, J. C., Jung, D., Wan, Y., and Bowers, J. E., "Perspective: The future of quantum dot photonic integrated circuits," *APL Photonics* **3**(3), 030901 (2018).

[3] Cox, C. H., Ackerman, E. I., Betts, G. E., and Prince, J. L., "Limits on the performance of RF-over-fiber links and their impact on device design," *IEEE Transactions on Microwave Theory and Techniques* **54**(2), 906–920 (2006).

[4] Crowley, M. T., Naderi, N. A., Su, H., Grillot, F., and Lester, L. F., "GaAs-based quantum dot lasers," in [*Semiconductors and Semimetals*], **86**, 371–417, Elsevier (2012).

[5] Eisenstein, G. and Bimberg, D., [*Green Photonics and Electronics*], Springer (2017).
[6] Huang, H., Lin, L.-C., Chen, C.-Y., Arsenijević, D., Bimberg, D., Lin, F.-Y., and Grillot, F., "Multimode optical feedback dynamics in InAs/GaAs quantum dot lasers emitting exclusively on ground or excited states: transition from short-to long-delay regimes," *Optics Express* **26**(2), 1743–1751 (2018).
[7] Lin, L.-C., Chen, C.-Y., Huang, H., Arsenijević, D., Bimberg, D., Grillot, F., and Lin, F.-Y., "Comparison of optical feedback dynamics of InAs/GaAs quantum-dot lasers emitting solely on ground or excited states," *Optics Letters* **43**(2), 210–213 (2018).
[8] Sciamanna, M. and Shore, K. A., "Physics and applications of laser diode chaos," *Nature Photonics* **9**(3), 151 (2015).
[9] Lelarge, F., Dagens, B., Renaudier, J., Brenot, R., Accard, A., van Dijk, F., Make, D., Le Gouezigou, O., Provost, J.-G., Poingt, F., et al., "Recent advances on InAs/InP quantum dash based semiconductor lasers and optical amplifiers operating at 1.55 μm," *IEEE Journal of Selected Topics in Quantum Electronics* **13**(1), 111–124 (2007).
[10] Capua, A., Rozenfeld, L., Mikhelashvili, V., Eisenstein, G., Kuntz, M., Laemmlin, M., and Bimberg, D., "Direct correlation between a highly damped modulation response and ultra low relative intensity noise in an InAs/GaAs quantum dot laser," *Optics Express* **15**(9), 5388–5393 (2007).
[11] Liu, A. Y., Komljenovic, T., Davenport, M. L., Gossard, A. C., and Bowers, J. E., "Reflection sensitivity of 1.3 μm quantum dot lasers epitaxially grown on silicon," *Optics Express* **25**(9), 9535–9543 (2017).
[12] Pawlus, R., Breuer, S., and Virte, M., "Relative intensity noise reduction in a dual-state quantum-dot laser by optical feedback," *Optics Letters* **42**(21), 4259–4262 (2017).
[13] Hayau, J.-F., Besnard, P., Dehaese, O., Grillot, F., Piron, R., Loualiche, S., Martinez, A., Merghem, K., and Ramdane, A., "Effect of the wetting layer on intensity noise in quantum dot laser," in [*Optical Communication, 2009. ECOC'09. 35th European Conference on*], 1–2, IEEE (2009).
[14] Wang, C., Zhuang, J.-P., Grillot, F., and Chan, S.-C., "Contribution of off-resonant states to the phase noise of quantum dot lasers," *Optics Express* **24**(26), 29872–29881 (2016).
[15] Petermann, K., [*Laser diode modulation and noise*], vol. 3, Springer Science & Business Media (2012).
[16] Schuh, K., Gartner, P., and Jahnke, F., "Combined influence of carrier-phonon and coulomb scattering on the quantum-dot population dynamics," *Physical Review B* **87**(3), 035301 (2013).
[17] Duan, J., Huang, H., Lu, Z., Poole, P., Wang, C., and Grillot, F., "Narrow spectral linewidth in InAs/InP quantum dot distributed feedback lasers," *Applied Physics Letters* **112**(12), 121102 (2018).